Pergamon

Int. J. Solids Structures Vol. 31, No. 12/13, pp. 1777–1792, 1994
Elsevier Science Ltd
Printed in Great Britain
0020-7683/94 $7.00 + .00

0020-7683(93)E0015-A

A FIELD BOUNDARY ELEMENT FORMULATION FOR MATERIAL NONLINEAR PROBLEMS AT FINITE STRAINS

A. FOERSTER and G. KUHN
Lehrstuhl für Technische Mechanik, Egerlandstraße 5, D-91058 Erlangen, Germany

Abstract—A boundary element formulation for geometrical nonlinear problems is presented, which is applicable for arbitrary constitutive equations based on the concept of hyperelastic response relative to an intermediate configuration. This includes purely hyperelastic problems at large elastic strains. In contrast to other formulations, the Total-Lagrange framework employed in this work significantly increases the numerical efficiency as the system matrices remain constant during the incremental solution and have to be computed only once. A nonlinear set of equations with an identical structure for both boundary and internal unknowns is derived. The basic unknowns are displacement gradients, which are calculated via integral equations and not by differentiation of the shape functions. The formulation can be consistently linearised to allow for the implementation of efficient iteration schemes using gradients, e.g. the Newton–Raphson scheme.

1. INTRODUCTION

The boundary element method (BEM) is now well established for geometrically linear problems for both elastic and inelastic material behaviour. As the presence of nonlinearities accounts for an additional domain integral, the term "field boundary element method" (FBEM) is frequently used in this context. Only a few papers can be found in the literature which are concerned with the application of FBEM to geometrical and material nonlinear problems [see e.g. Chandra and Mukherjee (1986a,b), Chen and Ji (1989, 1990), Jin *et al.* (1988, 1989), Mukherjee and Chandra (1984), Novati and Brebbia (1982), Okada *et al.* (1988, 1989, 1990) and Tran-Cong *et al.* (1990)]. Most of the approaches presented in these papers are based on constitutive equations in rate form.† As a consequence, the whole system of FBEM equations takes on a rate form and must be time-integrated using incrementally objective algorithms. This recommends explicit integration schemes, which react quite sensitively with respect to the increment size. The more complicated formulation of implicit schemes or equilibrium iterations is mostly avoided and can only be found in Jin *et al.* (1988, 1989) to the knowledge of the authors. As an additional drawback for the derivation and implementation, such constitutive equations have to be formulated in terms of objective time derivatives of conjugate stress and strain measures.

The elastic part of deformation is usually assumed to be determined by a hypoelastic law with a constant and isotropic elasticity tensor. This is not compatible with reversible (hyperelastic) material behaviour in any configuration except the initial configuration [see e.g. Simo (1984)]. Nevertheless such hypoelastic laws are taken as a basis for FBEM approaches in an Updated-Lagrange framework for various configurations. Therefore the validity of such formulations is restricted to small elastic strains, whereas finite rotations are admissible as orthogonal transformations do not affect an isotropic elasticity tensor.

The application of an Updated-Lagrange framework is frequently enforced either by approximations or linearisations, which are admissible for small strain increments between two related configurations, or by a derivation based on an analogy of Betti's reciprocal theorem for small strain increments superimposed onto a finitely deformed configuration. The main drawback of this procedure is the fact that the system matrices have to be re-computed after each load increment if the configuration has changed significantly. This is

† Exceptions are Tran-Cong *et al.* (1990) using hyperelastic constitutive equations and Novati and Brebbia (1982) using Saint-Venant's law, which is not polyconvex and therefore restricted to small elastic strains.

numerically much more time-consuming than the re-computation of the stiffness-matrix in FEM.

Some of these drawbacks can be overcome by the proposed approach. The main point is the application of constitutive equations based on the concept of an intermediate configuration. This enables the decomposition of the set of constitutive equations into a simple hyperelastic relation for the stress tensor and more complicated evolution equations for the intermediate configuration and further internal variables. Such constitutive models are well justified from a thermodynamic point of view [see e.g. Coleman and Gurtin (1967), Lubliner (1984)] and are widely used in FEM [see e.g. Besdo (1981), Simo (1988a,b), Simo and Miehe (1992), Miehe *et al.* (1992) and Eterovic and Bathe (1990)]. The stresses can be calculated directly from kinematic quantities, and the problem can be regarded as strain-driven. This allows for a time-independent formulation on a global level; whereas the integration of the evolution equations is performed on a nodal level.

It will be shown that such constitutive models, covering elastoplastic, viscoplastic and thermo-elastoplastic problems [see e.g. Simo (1988a,b), Simo and Miehe (1992), Miehe and Stein (1992)] are suitable for an implementation in FBEM schemes. This includes (as a special case) the efficient treatment of hyperelasticity at finite strains, even for incompressible materials [see Foerster and Kuhn (1993)]. It deserves mentioning that no approximations concerning the basic equations are necessary to establish a Total-Lagrange-FBEM formulation, which is properly based on finite strain continuum mechanics. The derivation starts from the weak form of the balance of linear momentum. Suitably defined nonlinear terms are separated after the first integration by parts, giving rise to an additional domain integral. The remaining terms can undergo the classical BEM-derivation using Kelvin's fundamental solution. The separation of linear and nonlinear terms is in some sort artificial but nevertheless exact and leads to a remarkably simple structure of the kernel in the additional domain integral.

A standard discretisation procedure and some further manipulations finally lead to a time-independent nonlinear set of equations with the displacement gradients at the nodes of all internal cells as basic unknowns. The structure of the set of nonlinear equations is identical for both boundary and internal values of the displacement gradients. It has to be solved in a combination with the integration algorithms of the evolution equations. In contrast to other approaches which differentiate the shape functions as in FEM, the displacement gradients are computed here via integral equations. The boundary tractions and the boundary or internal displacements can be computed in a post-processing procedure once the displacement gradients have been determined. The nonlinear set of equations is suitable for consistent linearisation, an important feature with regard to the application of efficient iterative solution techniques. The linearisation is quite simple and requires little effort from a computational point of view. It involves the computation of consistent material tangent moduli analogous to the proceeding in FEM.

In this approach the system matrices remain constant and the linearisation procedure only affects simple nonlinear functions on a nodal level. This is in contrast to FEM-formulations, where the discretised integral representation of the tangent stiffness matrix contains the material tangent moduli due to the underlying variational structure. As a consequence the re-computation of the stiffness matrix requires a complete domain integration in each iteration step† which can be completely avoided in the present formulation.

2. GOVERNING EQUATIONS

For the sake of simplicity the notation of classical tensor analysis is adopted. The concept of manifolds, set up for example by Marsden and Hughes (1983) in the context of finite elasticity and widely adopted in the literature, has no significant advantage for our purposes. As the problem is treated in a Total-Lagrange framework, the basic equations will be mainly given in a material formulation.

† Update schemes (e.g. BFGS, DFP) or modified Newton–Raphson schemes can overcome this problem in part.

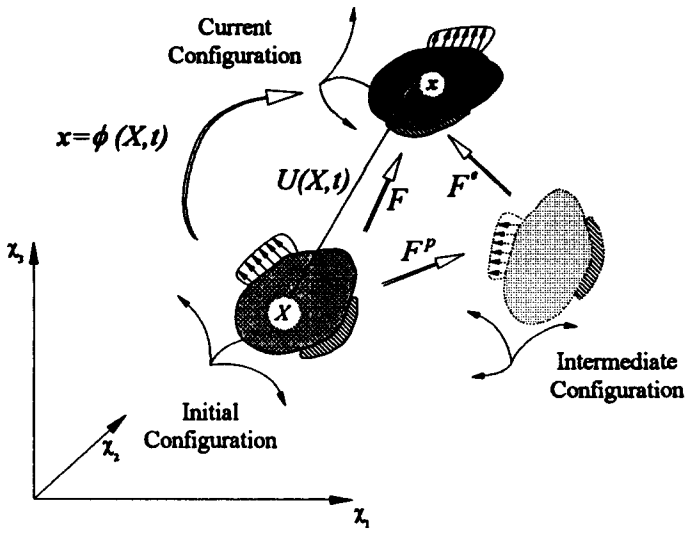

Fig. 1. Configurations, displacements and deformation gradients.

The deformation of a body from the initial to the current configuration can be described as an invertible mapping $x = \phi(X, t)$, relating the coordinates X and x of a material point in the initial and the current configuration, respectively, at a certain time t (see Fig. 1). The linearisation of this mapping

$$\mathbf{F} = \frac{\partial \phi^a}{\partial X^A} \mathbf{g}_a \otimes \mathbf{G}^A, \tag{1}$$

is the deformation gradient, which is a two-point tensor. It can be used to define Lagrangian tensors, e.g. the right Cauchy–Green tensor

$$\mathbf{C} = \mathbf{F}^T \cdot \mathbf{F}, \tag{2}$$

and the Green strain tensor

$$\mathbf{E} = \tfrac{1}{2}[\mathbf{C} - \mathbf{G}]. \tag{3}$$

In eqn (1) and eqn (3) $\mathbf{g}_a$ and $\mathbf{G}^A$ denote the contravariant and covariant basis in the current and initial configuration, respectively, and $\mathbf{G}$ the metric tensor in the initial configuration. Alternatively the deformation can be described in terms of displacements $\mathbf{U}(X, t)$ defined as a material vector field assigned to the points X and x in the cartesian embedding space. $\mathbf{F}$, $\mathbf{C}$ and $\mathbf{E}$ can be expressed via the material displacement gradient $\mathbf{H} = \nabla \mathbf{U}$ e.g.

$$\mathbf{C} = \mathbf{H} + \mathbf{H}^T + \mathbf{H}^T \cdot \mathbf{H} + \mathbf{G}. \tag{4}$$

The material balance of linear momentum takes the following local

$$DIV[\mathbf{F} \cdot \mathbf{S}] + \mathbf{B} \cdot \rho = 0, \tag{5}$$

or global

$$\int_\Gamma \mathbf{T}\,\mathrm{d}\Gamma + \int_\Omega \mathbf{B}\cdot\rho\,\mathrm{d}\Omega = 0 \quad \text{with } \mathbf{T} = \mathbf{F}\cdot\mathbf{S}\cdot\mathbf{N}, \tag{6}$$

form and is written in terms of the second Piola–Kirchhoff stress tensor $\mathbf{S}$, the boundary traction vector $\mathbf{T}$, the volume force density $\mathbf{B}\cdot\rho$ and the unit outward normal $\mathbf{N}$, each defined in the initial configuration. The balance of angular momentum requires the symmetry of the second Piola Kirchhoff stress tensor. The relations between $\mathbf{S}$ and $\mathbf{T}$ and their spatial counterparts $\boldsymbol{\sigma}$ (Cauchy stress tensor) and $\mathbf{t} = \boldsymbol{\sigma}\cdot\mathbf{n}$ (Cauchy traction vector) defined in the current configuration are

$$\mathbf{S} = J\mathbf{F}^{-1}\cdot\boldsymbol{\sigma}\cdot\mathbf{F}^{-T} \quad \text{with } J = \det\mathbf{F}, \tag{7}$$

and

$$\mathbf{T} = (\mathbf{H}+\mathbf{G})\cdot\mathbf{S}\cdot\mathbf{N} = \mathbf{t}\frac{\mathrm{d}a}{\mathrm{d}A}, \tag{8}$$

where the latter equation can be derived from Nanson's formula.

The introduction of an intermediate configuration in the sense of Lee (1969), obtained by a local relaxation to a stress-free state at fixed internal variables, leads to a local multiplicative decomposition

$$\mathbf{F} = \mathbf{F}^e\cdot\mathbf{F}^p, \tag{9}$$

of the deformation gradient into an elastic and plastic† part. The decomposition is not unique in the sense that $\mathbf{F}^e$ and $\mathbf{F}^p$ are determined up to an orthogonal tensor only, whereas the plastic right Cauchy–Green tensor

$$\mathbf{C}^p = \mathbf{F}^{pT}\cdot\mathbf{F}^p, \tag{10}$$

is unique and objective. Thermodynamic considerations and the requirement of objectivity finally lead to a dependence of the free energy ψ from $\mathbf{C}$, $\mathbf{C}^p$ and further internal variables α and to the relation

$$\mathbf{S} = 2\rho\frac{\partial}{\partial\mathbf{C}}\psi(\mathbf{C}, \mathbf{C}^p, \boldsymbol{\alpha}), \tag{11}$$

for the second Piola–Kirchhoff stress tensor‡ [see e.g. Lubliner (1984, 1987), Coleman and Gurtin (1967) or Simo (1988a,b) for a detailed discussion]. This constitutive equation is accomplished by a set of evolution equations

$$\begin{aligned}\dot{\mathbf{C}}^p &= \mathscr{F}(\mathbf{C}, \mathbf{C}^p, \boldsymbol{\alpha}, \dot{\mathbf{C}})\\ \dot{\boldsymbol{\alpha}} &= \mathscr{G}(\mathbf{C}, \mathbf{C}^p, \boldsymbol{\alpha}, \dot{\mathbf{C}}),\end{aligned} \tag{12}$$

for the plastic right Cauchy–Green tensor and the internal variables.

The algorithmic integration of the evolution equations and the computation of the consistent material tangent moduli depend on the explicit structure of eqn (12) and affect the efficiency of the whole scheme. In Simo (1988a,b) or Simo and Miehe (1992) a constitutive model based on a Neo–Hookean hyperelastic relation, the von Mises yield condition and the principle of maximum plastic dissipation is proposed. It is widely used in FEM approaches as—in a spatial formulation—it allows for the derivation of radial-return algorithms analogous to the geometrical linear case and the closed-form representation of

† In a more general sense it should be called "inelastic".

‡ The dependence on the temperature can be dropped in a purely mechanical theory.

the consistent material tangent moduli. In order to use these efficient algorithms in a Total-Lagrange approach, the relevant (nodal) quantities have to be transformed via push-forward and pull-back operations from the initial to the current configuration and *vice versa*. The computational effort for this procedure is irrelevant in comparison with the iteration scheme as a whole. Alternatively, less efficient integration algorithms for arbitrary evolution equations can be used, which can be directly formulated in the initial configuration [e.g. cutting-plane or closest-point-projection algorithm, see Simo (1988a,b) and the references herein]. Further reading on this topic as well as on different approaches can be found for example in Besdo (1981), Eterovic and Bathe (1990), Lubliner (1984), Haupt (1985) and Miehe and Stein (1992).

3. FIELD BOUNDARY ELEMENT FORMULATION

For the derivation of a FBEM formulation it is necessary to express the relevant equations of the previous section in the following modified form

$$\begin{aligned} \mathbf{E} &= \tfrac{1}{2}[\mathbf{H}^T+\mathbf{H}]+\tfrac{1}{2}\mathbf{H}^T\cdot\mathbf{H} \\ 0 &= DIV[(\mathbf{G}+\mathbf{H})\cdot\mathbf{S}]+\mathbf{B}\cdot\rho \\ \mathbf{S} &= \hat{\mathbf{C}}:\mathbf{E}+\mathbf{S}^n. \end{aligned} \tag{13}$$

These equations can be obtained from eqns (3), (5) and (11) substituting the Green strain tensor by the material displacement gradient and formally splitting eqn (11) into linear and nonlinear parts. The latter involves the definition of a constant elasticity tensor

$$\hat{\mathbf{C}} = 4\rho\partial^2\psi/\partial\mathbf{C}^2|_{C=C^p=G} \tag{14}$$

resulting from the linearisation of eqn (11) for the undeformed state. The definition

$$\mathbf{S}^n = 2\rho\frac{\partial\psi}{\partial\mathbf{C}} - \hat{\mathbf{C}}:\mathbf{E}, \tag{15}$$

of the nonlinear stress tensor is suitably chosen to ensure the equivalence of eqn (13c) and the hyperelastic relation eqn (11). The more or less artificially defined "nonlinear stress tensor" $\mathbf{S}^n$ will be removed from the formulation later on. The elasticity tensor $\hat{\mathbf{C}}$ is assumed to be isotropic and homogeneous and can be written as

$$\hat{C}^{ABCD} = \frac{2Gv}{1-2v}G^{AB}G^{CD}+G(G^{AC}G^{BD}+G^{AD}G^{BC}), \tag{16}$$

in terms of the shear modulus G and the Poisson ratio v. If the material is inhomogeneous or initially anisotropic (i.e. ψ is not an isotropic tensor function of $\mathbf{C}$) a suitable averaging procedure should be used to define $\hat{\mathbf{C}}$ homogeneous and isotropic,† whereas the inhomogeneity and initial anisotropy of the real material are shifted to the nonlinear stress tensor. Material anisotropy arising from inelastic deformations is included in the nonlinear stress tensor, too.

Equations (13a–c) allow for the separation of nonlinear terms in such a way that the remaining terms have the same structure as the corresponding ones in linear elasticity. Therefore the well-known fundamental solutions of linear elasticity can be applied directly.

In order to keep the notation of the previous section, the relevant integral equations will be derived in arbitrary curvilinear coordinates in the initial configuration, although this is not necessary in general. The starting point is the weak form

† Alternatively, fundamental solutions for anisotropic linear elasticity could be employed, see e.g. Vogel and Rizzo (1973).

$$\int_\Omega \tilde{\mathbf{U}} \cdot \{DIV[(\mathbf{H}+\mathbf{G})\cdot\mathbf{S}]+\mathbf{B}\cdot\rho\}\,d\Omega = 0, \tag{17}$$

of the balance of linear momentum eqn (13b). The test function is chosen to be Kelvin's fundamental solution

$$\tilde{\mathbf{U}} = \tilde{\mathbf{B}}\cdot\overset{*}{\mathbf{U}} \quad \text{with } \overset{*}{\mathbf{U}} = \frac{1}{16\pi(1-\nu)Gr}\{(3-4\nu)\mathbf{G}+\nabla r\otimes\nabla r\}, \tag{18}$$

of Navier's equation of linear elasticity

$$DIV(\nabla\tilde{\mathbf{U}})+\frac{1}{1-2\nu}\nabla(DIV\tilde{\mathbf{U}})+\frac{1}{G}\tilde{\mathbf{B}}\delta(X,\xi) = 0 \tag{19}$$

for a unit load in infinite space, represented by the product of Dirac's function $\delta(X, \xi)$ and a constant vector $\tilde{\mathbf{B}}$. The material parameters G and ν in eqns (18) and (19) correspond to those used in eqn (16). The gradients (covariant derivatives) of the displacement field

$$\nabla\tilde{\mathbf{U}} = \tilde{\mathbf{B}}\cdot\nabla\overset{*}{\mathbf{U}}, \quad \nabla_\xi\tilde{\mathbf{U}} = \tilde{\mathbf{B}}\cdot\nabla_\xi\overset{*}{\mathbf{U}}, \quad \nabla_\xi(\nabla\tilde{\mathbf{U}}) = \tilde{\mathbf{B}}\cdot\nabla_\xi(\nabla\overset{*}{\mathbf{U}}) \tag{20}$$

with respect to the field point and the source point coordinates, respectively, and the stresses and boundary tractions

$$\tilde{\mathbf{\Sigma}} = \hat{\mathbf{C}}:\nabla\tilde{\mathbf{U}}, \quad \tilde{\mathbf{T}} = \mathbf{\Sigma}\cdot\mathbf{N} = \tilde{\mathbf{B}}\cdot\overset{*}{\mathbf{T}} \tag{21}$$

of the fundamental solution can be derived from $\tilde{\mathbf{U}}$. In eqn (18) r denotes the Euclidian norm of the vector associated to X and ξ in the cartesian embedding space, i.e. the "distance" between X and ξ. For Cartesian coordinates eqn (18) is reducible to the standard component representation. After a first integration by parts eqn (17) takes the form

$$0 = \int_\Gamma \tilde{\mathbf{U}}\cdot(\mathbf{G}+\mathbf{H})\cdot\mathbf{S}\cdot\mathbf{N}\,d\Gamma - \int_\Omega \nabla\tilde{\mathbf{U}}:[(\mathbf{G}+\mathbf{H})\cdot\mathbf{S}]\,d\Omega + \int_\Omega \tilde{\mathbf{U}}\cdot\mathbf{B}\cdot\rho\,d\Omega. \tag{22}$$

The last domain integral containing the volume forces will not be considered in the following.† Inserting the definition of the traction vector eqn (8) into the boundary integral of eqn (22), one obtains

$$\int_\Gamma \tilde{\mathbf{U}}\cdot(\mathbf{G}+\mathbf{H})\cdot\mathbf{S}\cdot\mathbf{N}\,d\Gamma = \int_\Gamma \tilde{\mathbf{U}}\cdot\mathbf{T}\,d\Gamma, \tag{23}$$

as its final form. Now the nonlinear terms in the remaining domain integral of eqn (22) can be separated using eqns (13a–c), causing additional domain integrals. First the transformation

$$\int_\Omega \nabla\tilde{\mathbf{U}}:[(\mathbf{G}+\mathbf{H})\cdot\mathbf{S}]\,d\Omega = \int_\Omega \nabla\tilde{\mathbf{U}}:\mathbf{S}\,d\Omega + \int_\Omega \nabla\tilde{\mathbf{U}}:(\mathbf{H}\cdot\mathbf{S})\,d\Omega, \tag{24}$$

shifts the nonlinear part of the balance of linear momentum to the second domain integral on the right-hand side. Next the nonlinear stresses are separated via

† For conservative volume forces it can be transformed into a boundary integral, see for example, Stippes and Rizzo (1977).

$$\int_\Omega \nabla\tilde{\mathbf{U}} : \mathbf{S}\, d\Omega = \int_\Omega \nabla\tilde{\mathbf{U}} : \hat{\mathbf{C}} : \mathbf{E}\, d\Omega + \int_\Omega \nabla\tilde{\mathbf{U}} : \mathbf{S}^n\, d\Omega. \tag{25}$$

Separating the quadratic term of the Green strain tensor one can derive

$$\int_\Omega \nabla\tilde{\mathbf{U}} : \hat{\mathbf{C}} : \mathbf{E}\, d\Omega = \int_\Omega \tilde{\boldsymbol{\Sigma}} : \mathbf{H}\, d\Omega + \int_\Omega \tfrac{1}{2}\tilde{\boldsymbol{\Sigma}} : (\mathbf{H}^T \cdot \mathbf{H})\, d\Omega \tag{26}$$

for the first domain integral on the right-hand side of eqn (25), using the symmetry properties of $\hat{\mathbf{C}}$ due to its definition as second order derivative of the free energy [eqn (14)]. The remaining domain integral can be integrated by parts again to obtain

$$\begin{aligned}\int_\Omega \tilde{\boldsymbol{\Sigma}} : \mathbf{H}\, d\Omega &= \int_\Gamma \mathbf{U} \cdot \tilde{\mathbf{T}}\, d\Gamma - \int_\Omega \mathbf{U} \cdot DIV(\tilde{\boldsymbol{\Sigma}})\, d\Omega \\ &= \int_\Gamma \mathbf{U} \cdot \tilde{\mathbf{T}}\, d\Gamma + \int_\Omega \mathbf{U} \cdot \tilde{\mathbf{B}}\, \delta(X, \xi)\, d\Omega,\end{aligned} \tag{27}$$

in which the balance of linear momentum of the fundamental solution was inserted. For $\xi \in \Omega$ the last domain integral of eqn (27) is reducible to $\mathbf{U}(\xi) \cdot \tilde{\mathbf{B}}$. After the insertion of eqns (23)–(27) into eqn (22) and the substitution of the displacements, displacement gradients and boundary tractions of the fundamental solution as given in eqns (18), (20) and (21), one obtains the generalized Somigliana identity

$$\begin{aligned}\mathbf{U}(\xi) = \int_\Gamma [\dot{\mathbf{U}}(X, \xi) \cdot \mathbf{T}(X) - \dot{\mathbf{T}}(X, \xi) \cdot \mathbf{U}(X)]\, d\Gamma + \int_\Omega \dot{\mathbf{U}}(X, \xi) \cdot \mathbf{B}(X)\rho(X)\, d\Omega \\ - \int_\Omega \nabla\dot{\mathbf{U}}(X, \xi) : \mathbf{NI}(X)\, d\Omega,\end{aligned} \tag{28}$$

for this problem. The three additional domain integrals were summed up in one defining the nonlinear expression

$$\mathbf{NI} = \mathbf{H} \cdot \mathbf{S} + \tfrac{1}{2}\hat{\mathbf{C}} : [\mathbf{H}^T \cdot \mathbf{H}] + \mathbf{S}^n = [\mathbf{H} + \mathbf{G}] \cdot \mathbf{S} - \hat{\mathbf{C}} : \mathbf{H}, \tag{29}$$

where the nonlinear stress tensor is removed from **NI** and from the entire formulation by inserting its definition eqn (15). In the limiting case of small displacement gradients and in the absence of plastic strains **NI** converges to zero of a higher order than the other kernels. In this case the additional domain integral vanishes, and the classical boundary integral equation for linear elasticity is recovered.

The standard limiting process $\xi \to \Gamma$ applied to eqn (28) finally provides the generalized boundary integral equation

$$\begin{aligned}\tilde{\mathbf{C}}(\xi) \cdot \mathbf{U}(\xi) = \int_\Gamma [\dot{\mathbf{U}}(X, \xi) \cdot \mathbf{T}(X) - \dot{\mathbf{T}}(X, \xi) \cdot \mathbf{U}(X)]\, d\Gamma + \int_\Omega \dot{\mathbf{U}}(X, \xi) \cdot \mathbf{B}(X)\rho(X)\, d\Omega \\ - \int_\Omega \nabla\dot{\mathbf{U}}(X, \xi) : \mathbf{NI}(X)\, d\Omega\end{aligned} \tag{30}$$

with a second order tensor $\tilde{\mathbf{C}}$ depending on the shape of Γ at ξ. At this stage the functional dependencies of **NI** have to be discussed. Taking into account eqn (11) the nonlinear expression **NI** takes the form

$$\mathbf{Nl}(\mathbf{H}, \mathbf{S}(\mathbf{C}, \mathbf{C}^p, \boldsymbol{\alpha})) = [\mathbf{H}+\mathbf{G}]\cdot\mathbf{S}(\mathbf{C}, \mathbf{C}^p, \boldsymbol{\alpha}) - \hat{\mathbf{C}} : \mathbf{H}. \tag{31}$$

The right Cauchy–Green tensor can be expressed directly in terms of $\mathbf{H}$, see eqn (4). The plastic right Cauchy–Green tensor $\mathbf{C}^p$ and the internal variables $\boldsymbol{\alpha}$ enter the formulation through the constitutive equation for the second Piola–Kirchhoff stress tensor.

The direct and indirect dependence of $\mathbf{Nl}$ on $\mathbf{H}$ requires a representation formula for the displacement gradient. For $\xi \in \Omega$ it can be easily obtained in an integral form by covariant differentiation of eqn (28) with respect to the source point coordinates ξ. Using the standard procedure, for example that given in Brebbia *et al.* (1984), one obtains

$$\mathbf{H}(\xi) = \nabla_\xi \mathbf{U}(\xi) = \int_\Gamma [\nabla_\xi \overset{*}{\mathbf{U}}(X, \xi)\cdot\mathbf{T}(X) - \nabla_\xi \overset{*}{\mathbf{T}}(X, \xi)\cdot\mathbf{U}(X)]\, d\Gamma$$

$$+ \int_\Omega \nabla_\xi \overset{*}{\mathbf{U}}(X, \xi)\cdot\mathbf{B}(X)\rho(X)\, d\Omega - \int_\Omega \nabla_\xi \nabla \overset{*}{\mathbf{U}}(X, \xi) : \mathbf{Nl}(X)\, d\Omega - \mathbf{F} : \mathbf{Nl}(\xi), \tag{32}$$

with a free term $\mathbf{F}$, explicitly given for example in Okada *et al.* (1989). The evaluation of the additional domain integral in eqns (30) and (32) in a discretised form usually requires the values of $\mathbf{Nl}$ and $\mathbf{H}$ in the domain Ω and on the boundary Γ, respectively.† The limiting process $\xi \to \Gamma$ applied to eqn (32) leads to a hypersingular boundary integral equation. The treatment of such integral equations is discussed, for example in Hildenbrand and Kuhn (1988), Bialecki *et al.* (1993) or Guiggiani *et al.* (1992) and will not be considered here.

4. DISCRETISATION

For the discretisation of eqns (30) and (32) the usual standard procedures are applied. The introduction of shape functions Φ and nodal values allows for the discretisation, for example, of the boundary integral equation

$$\begin{aligned}
\tilde{\mathbf{C}}(\xi)\cdot\mathbf{U}(\xi) = {} & \sum_{i=1}^{r}\sum_{k=1}^{n} \int_{\Gamma_{(i)}} \overset{*}{\mathbf{U}}(\xi, X(\eta))\cdot[\mathbf{T}_{(ik)}\overset{t}{\Phi}_{(k)}(\eta)] J(X, \eta)\, d\Gamma(\eta) \\
& - \sum_{i=1}^{r}\sum_{k=1}^{n} \int_{\Gamma_{(i)}} \overset{*}{\mathbf{T}}(\xi, X(\eta))\cdot[\mathbf{U}_{(ik)}\overset{u}{\Phi}_{(k)}(\eta)] J(X, \eta)\, d\Gamma(\eta) \\
& + \sum_{j=1}^{s}\sum_{l=1}^{m} \int_{\Omega_{(j)}} \overset{*}{\mathbf{U}}(\xi, X(\zeta))\cdot[\rho\mathbf{B}_{(jl)}\overset{b}{\Phi}_{(l)}(\eta)] J(X, \zeta)\, d\Omega(\zeta) \\
& - \sum_{j=1}^{s}\sum_{l=1}^{m} \int_{\Omega_{(j)}} \nabla \overset{*}{\mathbf{U}}(\xi, X(\zeta)) : [\mathbf{Nl}_{(jl)}\overset{n}{\Phi}_{(l)}(\eta)] J(X, \zeta)\, d\Omega(\zeta).
\end{aligned} \tag{33}$$

The boundary tractions $\mathbf{T}$ and displacements $\mathbf{U}$ are approximated in r boundary elements with $n(r)$ nodes each, and the nonlinear term $\mathbf{Nl}$ in s internal cells with $m(s)$ nodes each. The standard collocation, Galerkin or least-square techniques applied to the discretised integral equations then provide the matrix equations

$$\mathbf{Au} = \mathbf{Bt} + \mathbf{b} - \mathbf{En} \to \tilde{\mathbf{A}}\mathbf{x} = \tilde{\mathbf{B}}\mathbf{y} + \mathbf{b} - \mathbf{En}, \tag{34}$$

and

$$\mathbf{h} = \tilde{\mathbf{G}}\mathbf{y} + \tilde{\mathbf{H}}\mathbf{x} + \tilde{\mathbf{b}} - \mathbf{E}'\mathbf{n}. \tag{35}$$

The vectors $\mathbf{u}$, $\mathbf{t}$, $\mathbf{y}$ and $\mathbf{x}$ contain the values of the boundary displacements and tractions

† The need to determine displacement gradients on the boundary can be avoided using constant or discontinuous elements.

and the known and unknown boundary values, respectively, for the nodes of boundary elements. The vectors $\mathbf{h}$ and $\mathbf{n}$, on the other hand, contain the values of $\mathbf{H}$ and $\mathbf{Nl}$ for the nodes of the internal cells. Inserting eqn (34b) into eqn (35) a nonlinear set of equations

$$0 = \mathbf{f} = \mathbf{h} + \tilde{\mathbf{E}}\mathbf{n} - \overset{(I)}{\mathbf{h}}(\lambda), \tag{36}$$

with a residual vector $\mathbf{f}$ can be obtained, where

$$\tilde{\mathbf{E}} = [\tilde{\mathbf{H}}\tilde{\mathbf{A}}^{-1}\mathbf{E} + \mathbf{E}'], \tag{37}$$

is a constant matrix and

$$\overset{(I)}{\mathbf{h}}(\lambda) = [\tilde{\mathbf{H}}\tilde{\mathbf{A}}^{-1}\tilde{\mathbf{B}} + \tilde{\mathbf{G}}]\mathbf{y}(\lambda) + \tilde{\mathbf{H}}\tilde{\mathbf{A}}^{-1}\mathbf{b} + \tilde{\mathbf{b}}, \tag{38}$$

is the vector of "linear" displacement gradients, which can be directly computed from the prescribed boundary values and volume forces once the system matrices have been computed. It represents the "external loading" in eqn (38) as a function of a loading parameter λ.

5. CONSISTENT LINEARISATION AND ITERATIVE SOLUTION

The path-dependence of inelastic problems requires an incremental solution strategy for eqn (36) taking into account the integration algorithms of the evolution equations. Even for hyperelastic problems an incremental approach in the sense of a path-following method is frequently required due to the strong nonlinearity of the problem, i.e. convergence is usually not obtained for the entire loading applied in one increment.† The situation in the typical $(k+1)$st load increment may be summarized as follows:

One has to determine $\mathbf{h}^{k+1}$ as the solution of

$$\mathbf{f}^{k+1} = \mathbf{h}^{k+1} + \tilde{\mathbf{E}}\mathbf{n}(\mathbf{h}^{k+1}, \mathbf{s}(\mathbf{c}^{k+1}, \mathbf{c}^{p^{k+1}}, \boldsymbol{\alpha}^{k+1})) - \overset{(I)}{\mathbf{h}}{}^{k+1} = 0 \tag{39}$$

in which $\mathbf{c}^{k+1}$ is a function of $\mathbf{h}^{k+1}$ and the components of $\mathbf{c}^{p^{k+1}}$ and $\boldsymbol{\alpha}^{k+1}$ result from time-discrete integration algorithms of the evolution equations symbolically written as

$$\begin{aligned} \mathbf{C}^{p^{k+1}} &= \hat{\mathscr{F}}(\mathbf{C}^{k+1}, (\mathbf{C}, \mathbf{C}^p, \alpha)^k) \\ \boldsymbol{\alpha}^{k+1} &= \hat{\mathscr{G}}(\mathbf{C}^{k+1}, (\mathbf{C}, \mathbf{C}^p, \alpha)^k). \end{aligned} \tag{40}$$

The integration starts from known nodal values $(\mathbf{C}, \mathbf{C}^p, \boldsymbol{\alpha})^k$ at the end of the kth load increment to avoid influences of the iteration path. The vector $\mathbf{h}^{(I)k+1}$ represents the new loading in the $(k+1)$st load increment.

Most existing FBEM approaches use fixed point iteration schemes not requiring gradients. In some cases this is enforced by the fact that both boundary integral equations and Somigliana-like identities for internal points are used parallel in an iterative procedure instead of constructing a set of equations with a unique structure. Fixed point iterations or similar schemes can be very efficient for moderately nonlinear problems, e.g. small strain elastoplasticity, whereas applied to highly nonlinear ones, they exhibit poor convergence properties or even fail to converge. Such problems are reported e.g. in Tran-Cong *et al.* (1990) in the context of a FBEM formulation for hyperelasticity at finite strains. The application of advanced iteration schemes is recommended in such cases. This means that the linearisation of the nonlinear problem with respect to the basic unknowns is necessary.

† Bifurcation or instability problems require incremental procedures, too, but will not be considered here.

In this formulation the basic unknowns are the nodal displacement gradients summarized in **h**. The Jacobi matrix† is therefore given by

$$\mathbf{J} = \frac{\mathrm{d}\mathbf{f}}{\mathrm{d}\mathbf{h}} = \mathbf{I} + \tilde{\mathbf{E}}\frac{\mathrm{d}\mathbf{n}}{\mathrm{d}\mathbf{h}}. \tag{41}$$

The matrix $\mathrm{d}\mathbf{n}/\mathrm{d}\mathbf{h}$ is sparse, as a nodal value of **Nl** only depends from the value of **H** at the same node. Arranging the nodal components in **h** and **n** in the same manner, one arrives at the block diagonal structure

$$\frac{\mathrm{d}\mathbf{n}}{\mathrm{d}\mathbf{h}} = \mathrm{Diag}\left[\frac{\mathrm{d}\mathbf{Nl}_1}{\mathrm{d}\mathbf{H}_1}, \ldots, \frac{\mathrm{d}\mathbf{Nl}_n}{\mathrm{d}\mathbf{H}_n}\right] \tag{42}$$

in which the entries $(\mathrm{d}\mathbf{Nl}/\mathrm{d}\mathbf{H})_i$ have the dimension 9×9 (3D) or 4×4 (2D) and contain the components of

$$\frac{\mathrm{d}Nl^{AB}}{\mathrm{d}H^{C}{}_{D}} = \delta^{A}{}_{C}S^{BD} + [H^{A}{}_{E} + \delta^{A}{}_{E}]\frac{\mathrm{d}S^{EB}}{\mathrm{d}H^{C}{}_{D}} - \hat{C}^{ABGD}G_{GC}. \tag{43}$$

The block diagonal structure of $\mathrm{d}\mathbf{n}/\mathrm{d}\mathbf{h}$ reduces substantially the numerical effort for the evaluation of eqn (41). After substituting the relation

$$\frac{\mathrm{d}S^{EB}}{\mathrm{d}H^{C}{}_{D}} = 2\frac{\mathrm{d}S^{EB}}{\mathrm{d}C_{DF}}[H^{G}{}_{F} + \delta^{G}{}_{F}]G_{GC} = \hat{C}^{ep^{EBDF}}[H^{G}{}_{F} + \delta^{G}{}_{F}]G_{GC}, \tag{44}$$

into eqn (43), it finally takes the form

$$\frac{\mathrm{d}Nl^{AB}}{\mathrm{d}H^{C}{}_{D}} = \delta^{A}{}_{C}S^{BD} + \{[H^{A}{}_{E} + \delta^{A}{}_{E}][H^{G}{}_{F} + \delta^{G}{}_{F}]\hat{C}^{ep^{EBDF}} - \hat{C}^{ABGD}\}G_{GC}, \tag{45}$$

with the consistent material tangent moduli $\hat{\mathbf{C}}^{ep}$. With these results at hand, the Newton–Raphson algorithm for the $(k+1)$st load increment:

Repeat

$$\begin{aligned}
&1)\ \mathbf{J}_n^{k+1} = [\mathrm{d}\mathbf{f}/\mathrm{d}\mathbf{h}]_n^{k+1}\\
&2)\ \mathbf{h}_{n+1}^{k+1} = \mathbf{h}_n^{k+1} - [\mathbf{J}_n^{k+1}]^{-1}\mathbf{f}_n^{k+1}\\
&3)\ \mathbf{c}_{n+1}^{p\,k+1} = \mathscr{F}(\mathbf{h}_{n+1}^{k+1}, (\mathbf{h}, \mathbf{c}^{p}, \boldsymbol{\alpha})^{k})\\
&4)\ \boldsymbol{\alpha}_{n+1}^{k+1} = \mathscr{G}(\mathbf{h}_{n+1}^{k+1}, (\mathbf{h}, \mathbf{c}^{p}, \boldsymbol{\alpha})^{k})\\
&5)\ \mathbf{s}_{n+1}^{k+1} = \mathscr{S}((\mathbf{c}, \mathbf{c}^{p}, \boldsymbol{\alpha})_{n+1}^{k+1})\\
&6)\ \mathbf{f}_{n+1}^{k+1} = \mathbf{h}_{n+1}^{k+1} + \tilde{\mathbf{E}}\mathbf{n}(\mathbf{h}_{n+1}^{k+1}, \mathbf{s}_{n+1}^{k+1}) - \mathbf{h}^{(I)k+1}
\end{aligned} \tag{46}$$

until $\|\mathbf{f}_{n+1}^{k+1}\| \leqslant \varepsilon$,

can be formulated as a simple example for iteration schemes using gradients. The steps in eqn (46) are the following:

1) Computation of the Jacobi matrix following the above scheme.
2) Calculation of an improved guess of the unknowns (displacement gradients).
3) Algorithmic integration of the evolution equation for $\mathbf{C}^{p}$ for all nodes.
4) Algorithmic integration of the evolution equation for $\boldsymbol{\alpha}$ for all nodes.
5) Direct computation of the stress tensors for all nodes via eqn (11).

† The counterpart in FEM is the tangent stiffness matrix.

6) Evaluation of eqn (36) to determine the new residual vector.

The iteration continues until a suitable norm of the residual vector is reduced to a certain tolerance.

Step 2 involves the solution of a large system of linear equations, which significantly accounts for the total computing time. As in FEM, update schemes can be used to overcome this problem at least in part. The consistent linearisation of eqn (11) for elastoplastic models with a yield condition provides either the actual elasticity tensor or the consistent elastoplastic tangent moduli. As the nodal state may change from the elastic domain to the yield surface or *vice versa* in a certain increment, the actual material response and its linearisation may not coincide at some nodes. In such situations the Jacobi matrix is not the correct linearisation of eqn (39) and the use of line-search algorithms in combination with the Newton–Raphson scheme is highly recommended to ensure convergence.

As a topic of further research solution techniques taking advantage of the diagonal dominance of the Jacobi matrix (not in a strictly mathematical sense) should be applied, e.g. iterative equation solvers in Newton–Raphson schemes or suitably adapted conjugate gradient methods. The application of algorithms to trace instability phenomena (e.g. arc-length methods) seems possible in general and has been successfully implemented and tested for hyperelastic problems, in which steps 3 and 4 are omitted and the consistent material tangent moduli in eqns (44) and (45) reduce to the actual elasticity tensor, which is different from the initial elasticity tensor defined in eqn (14).

6. IMPLEMENTATION AND NUMERICAL RESULTS

The formulation derived above was implemented in the boundary element program BEAT for two-dimensional problems, covering hyperelasticity and rate-independent associative elastoplasticity with interfaces for various hyperelastic relations and yield conditions. The constitutive model proposed in Simo (1988a,b) or Simo and Miehe (1992) (including the efficient algorithms given in these references) was implemented, too. Some additional features were not described in this paper† to ensure the clarity of the derivation, such as

- the easy treatment of hyperelastic materials with internal constraints (e.g. incompressibility) without causing locking phenomena like in FEM [see Foerster (1993)],
- the use of modified Newton–Raphson and update schemes (e.g. Broyden's rank one update) for hyperelastic problems to avoid the time-consuming re-factorization of the Jacobi matrix,
- the development and implementation of different types of line search algorithms to improve the numerical stability of the iteration scheme, especially for elastoplastic problems,
- the implementation of the substructuring technique to allow for the efficient treatment of bodies consisting of different materials and
- the treatment of nonlinear boundary conditions (e.g. traction vectors prescribed in the current configuration, pressure boundary conditions and traction vectors rotating with the tangent plane of the boundary) via a minor extension of the algorithm.

The computational examples presented in the following are plain strain problems. Some hyperelastic problems will be considered to assess the efficiency of the global time independent FBEM scheme. The interaction of this scheme with the local integration algorithms of the evolution equations will be discussed on the basis of two elastoplastic examples.

Two homogeneous deformations (simple shear and uniaxial extension or compression) of a rectangular plate, consisting of an incompressible rubberlike Mooney–Rivlin material,

† See Foerster (1993) for a detailed derivation.

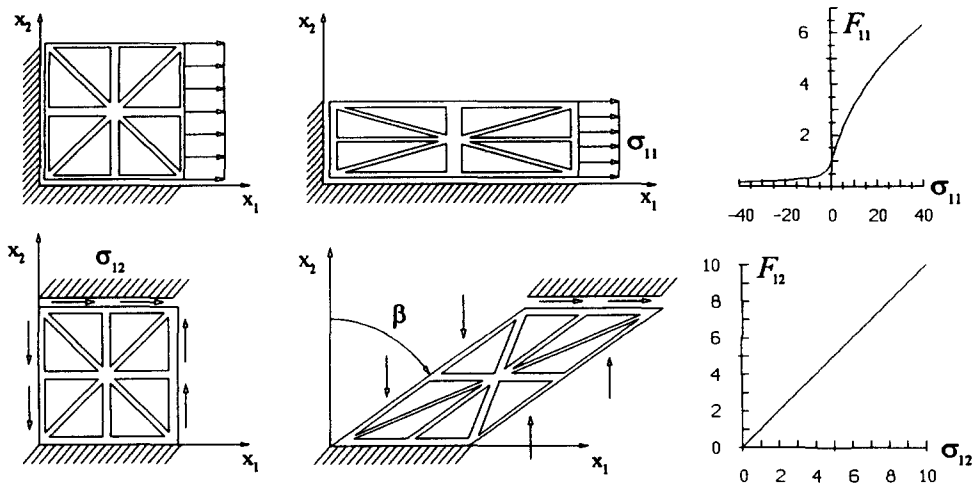

Fig. 2. Simple shear and uniaxial extension (compression).

will be considered (see Fig. 2). These deformations are characterized by the deformation gradients

$$\mathbf{F} = \underbrace{\begin{bmatrix} 1 & \gamma & 0 \\ 0 & 1 & 0 \\ 0 & 0 & 1 \end{bmatrix}}_{\text{Simple shear}} \quad (\text{with } \gamma = \tan\beta) \quad \text{and} \quad \mathbf{F} = \underbrace{\begin{bmatrix} 1+\delta & 0 & 0 \\ 0 & \dfrac{1}{1+\delta} & 0 \\ 0 & 0 & 1 \end{bmatrix}}_{\text{Uniaxial extension}}, \tag{47}$$

with the shearing angel β and the engineering strain δ. As the deformations are homogeneous, even a minimum number of linear boundary elements and constant internal cells would exactly represent the problem. Here eight linear boundary element and eight linear triangular cells were used, but coarse or refined meshes of course provided the same results. The kinematic constraints for both examples are shown in Fig. 2. The loading was imposed via boundary tractions, which is the more complicated case for the iterative solution compared with kinematic loading. The constraints on the upper side of the shear-specimen were applied to catch the normal stresses due to the Pointing effect, and the boundary tractions (obtained from the analytical solution) were prescribed as Cauchy tractions.† In the simple shear problem any hydrostatic pressure can be superimposed via suitably chosen boundary tractions on the vertical sides of the specimen, which do not remain tangential in general. The ranges of deformation (which are not the limiting values) and the average number of iterations per load increment required by different solution algorithms are given in Table 1 for 5, 10 and 20 equal load increments.‡ An extremely

Table 1. Average number of iterations for different solution schemes and different numbers of load increments

	Number of load increments								
	5	10	15	5	10	15	5	10	15
NR	4.0	3.7	3.6	5.2	4.3	4.2	6.8	5.2	4.8
M-NR and BR	28.4	18.9	14.0	18.8	11.8	9.2	X	21.1	14.4
M-NR	X	55.9	17.0	X	24.8	16.0	X	X	20.5
Range of deformation	Simple shear $0.0 \leqslant F_{12} \leqslant 3.0$			Extension $1.0 \leqslant F_{11} \leqslant 5.0$			Compression $1.0 \geqslant F_{11} \geqslant 0.2$		

NR: Newton–Raphson; M-NR: Modified Newton–Raphson; BR: Broyden rank one update; X: No convergence.

† This is an additional nonlinearity of the problem, as material traction vectors occur in the integral equations.

‡ An adaptive load increment control is recommended for less academic problems to save computing time.

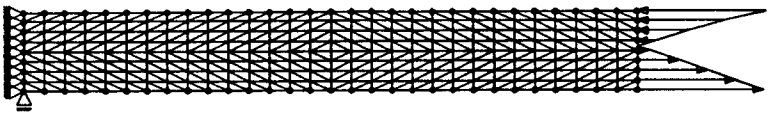

Fig. 3. Hyperelastic beam (discretisation).

stringent global error tolerance of $\|\mathbf{f}\| \leqslant 1.E\text{-}14$ was imposed for all load increments,† partly accounting for the number of iterations given in Table 1. The maximum absolute difference between the computed nodal deformation gradients and the analytical values is less than $5.E\text{-}8$ for all nodes and components. The restriction $(\sigma_{11}-\sigma_{22})-\gamma\sigma_{12}=0$ for the components of the Cauchy stress tensor, which is directly related to the Pointing effect for any incompressible hyperelastic material in simple shear, is preserved within an absolute tolerance of $6.E\text{-}6$. The modified Newton–Raphson scheme required one factorization of the initial Jacobi matrix in each load increment. The Broyden rank one update started from this factorization. The relative computational efficiency of the different solution schemes depends strongly on the size of the problem and has not yet been examined in detail. The low number of load increments and iterations proves the efficiency of both the formulation and the solution procedures for hyperelastic problems. As a limiting case a Newton–Raphson scheme with an additional line search solved the uniaxial extension problem up to 400% engineering strain in three load increments with a total of 19 iterations. For hyperelastic problems the numerical efficiency is significantly improved, if the components of the initial vector $\mathbf{h}_0^{k+1}$ in the $(k+1)$st increment are computed via extrapolation from the solutions of preceding load increments. This requires an adaptive choice of the increment size in combination with an error control scheme (the results in Table 1 were obtained without extrapolation).

The next example is the bending of a hyperelastic beam. The Mooney–Rivlin constitutive model for incompressible rubber-like materials was applied here. The boundary conditions and the discretisation with 76 isoparametric Overhauser-spline elements on the boundary, 480 linear internal cells and 279 nodes are shown in Fig. 3. At the right vertical side of the beam a resulting moment was applied by an appropriate distribution of tractions, which were defined relative to the rotating tangent of the boundary. The deformed configuration and contours of relevant components of the Cauchy stress tensor are shown in Fig. 4. The results are in good agreement with the solution to be expected for beam subjected to a constant bending moment only. A shift of the neutral axis to the inner radius is observed. The difference of the length of the neutral axis in the initial and the deformed

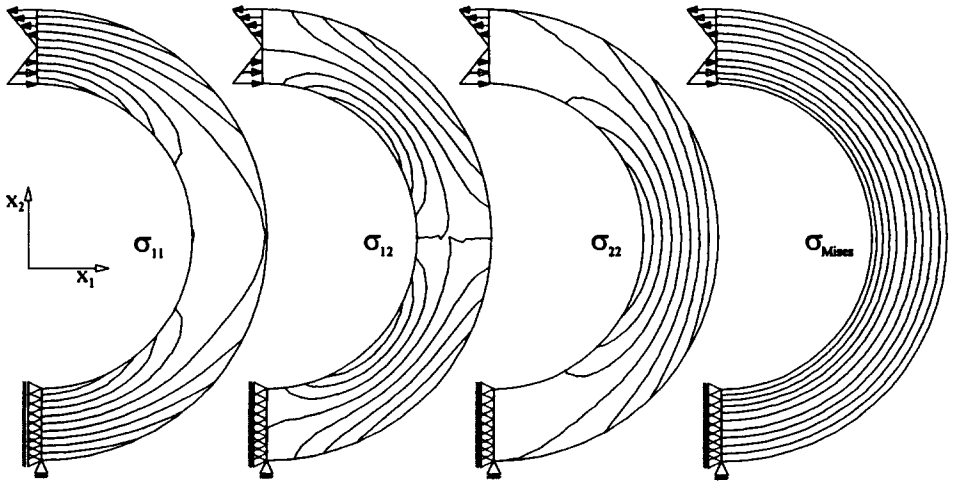

Fig. 4. Hyperelastic beam (contours of Cauchy stresses).

† All examples were computed with 64 bit precision.

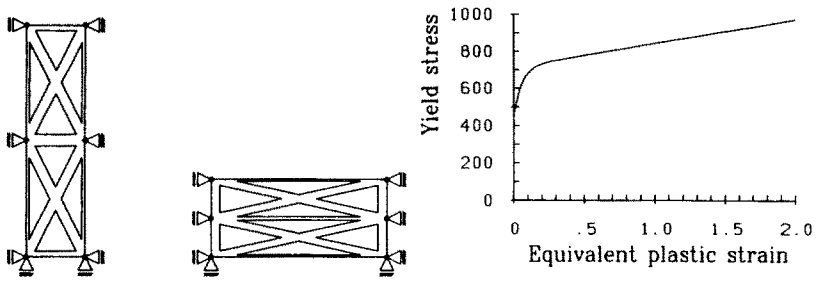

Fig. 5. Uniaxial elastoplastic extension.

configuration is 0.5%. The computation required 25 load increments with a total of 141 iterations, where a modified Newton–Raphson scheme with one factorization of the Jacobi matrix in each load increment was used. The error tolerance was set to $\|\mathbf{f}\| \leqslant 1.E\text{-}12$. It is worth mentioning again that the entire computation is carried out in the initial configuration. The effects of large rotations are correctly reproduced.

Next the uniaxial elastoplastic extension of a plate up to 200% engineering strain (which is again no limiting point of the algorithm) is examined, using the constitutive model (J_2-flow theory) proposed in Simo (1988a,b) with the isotropic exponential hardening law and the material data given herein. The shape of the undeformed plate is appropriately chosen to avoid bifurcation problems. The kinematic boundary conditions and the isotropic hardening law are shown in Fig. 5. In Table 2 the total number of iterations, the resulting stresses related to the initial yield stress Y_0 and the equivalent plastic strain are given for different numbers of load increments. The nodal stresses differ less than $1.E\text{-}4\ Y_0$ from each other, the equivalent plastic strains less than $1.E\text{-}7$. The solution technique applied here was the Newton–Raphson scheme. The small number of iterations even for large increments is due to the consistent linearisation of the problem, i.e. the use of consistent elastoplastic tangent moduli.

The last example is the extension of a rectangular plate with elliptical notches ($a/b = 3$) up to 25% engineering strain. The same constitutive model as in the previous example was used, but a linear hardening law (hardening coefficient: 7% of the bulk modulus) was applied, which is not a realistic assumption for large elastoplastic deformations. Using the realistic exponential hardening law proposed in Simo (1988a,b), the simulation points out the initiation of a localization process at an early stage of the deformation (5.0–5.5% engineering strain), which occurs about four boundary elements to the side of the symmetry line of the notches (see Fig. 6). Such phenomena can not be handled by the present implementation. The discretisation with 67 isoparametric Overhauser-spline elements on the boundary, 649 linear internal cells and 359 nodes is shown in Fig. 6. Due to the symmetry of the specimen only one quarter had to be considered. The problem was solved in 25 equal load increments with a total of 73 iterations for an error tolerance of $\|\mathbf{f}\| \leqslant 1.E\text{-}10$ by the Newton–Raphson algorithm with line search. The deformed configuration and contours of relevant components of the Cauchy stress tensor and the equivalent plastic strain are shown in Fig. 7.

Table 2. Results for uniaxial elastoplastic extension

	Number of load increments					
	1	2	4	8	16	32
Iterations	6	10	20	34	64	115
σ_{11}/Y_0	1.9140	2.1356	2.2160	2.2388	2.2447	2.2468
σ_{12}/Y_0	$<2.E\text{-}8$	$<2.E\text{-}8$	$<2.E\text{-}8$	$<2.E\text{-}8$	$<2.E\text{-}8$	$<2.E\text{-}8$
σ_{22}/Y_0	$<5.E\text{-}6$	$<5.E\text{-}6$	$<5.E\text{-}6$	$<5.E\text{-}6$	$<5.E\text{-}6$	$<5.E\text{-}6$
σ_{33}/Y_0	0.1913	0.6505	0.9007	1.0147	1.0671	1.0920
σ_V/Y_0	1.8259	1.8960	1.9303	1.9416	1.9447	1.9455
$\bar{\varepsilon}^p$	0.8376	1.0861	1.2078	1.2486	1.2596	1.2624

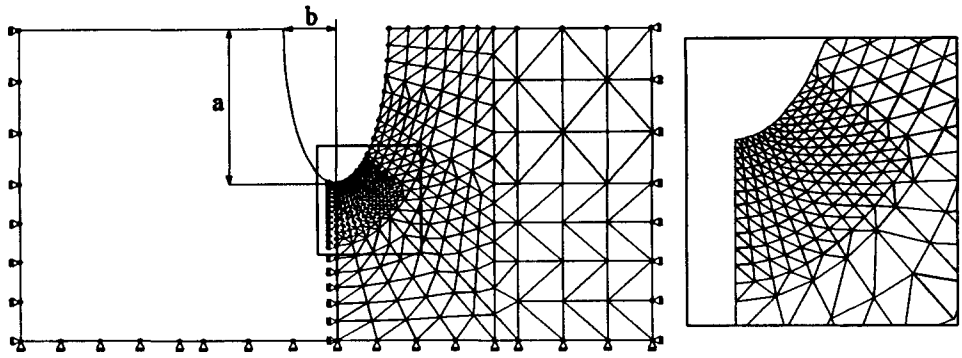

Fig. 6. Plate with elliptical notches (discretisation).

7. CONCLUSIONS

In this paper a finite strain FBEM formulation is presented, which is based on a class of constitutive equations not used in this context so far. It is shown that the concept of hyperelastic material behaviour relative to the intermediate configuration, covering a wide range of constitutive models, is especially suitable for an implementation in a FBEM scheme. It leads to a time-independent formulation on the global level and a remarkably simple structure of the kernel in the additional domain integral. Through this method the use of a Total-Lagrange scheme becomes possible, resulting in constant system matrices and a significant reduction of computing time. The application of advanced iterative solution schemes becomes possible, as the problem can be consistently linearised with little effort and without requiring any domain integration. In comparison with FEM-formulations, lower requirements on the discretisation quality can be expected for two reasons. Firstly, the quantities interpolated within the internal cells are functions of the displacement gradient and not functions of the displacements as in FEM. Secondly, no differentiation of the shape functions is necessary, as the displacement gradients can be computed via integral equations.

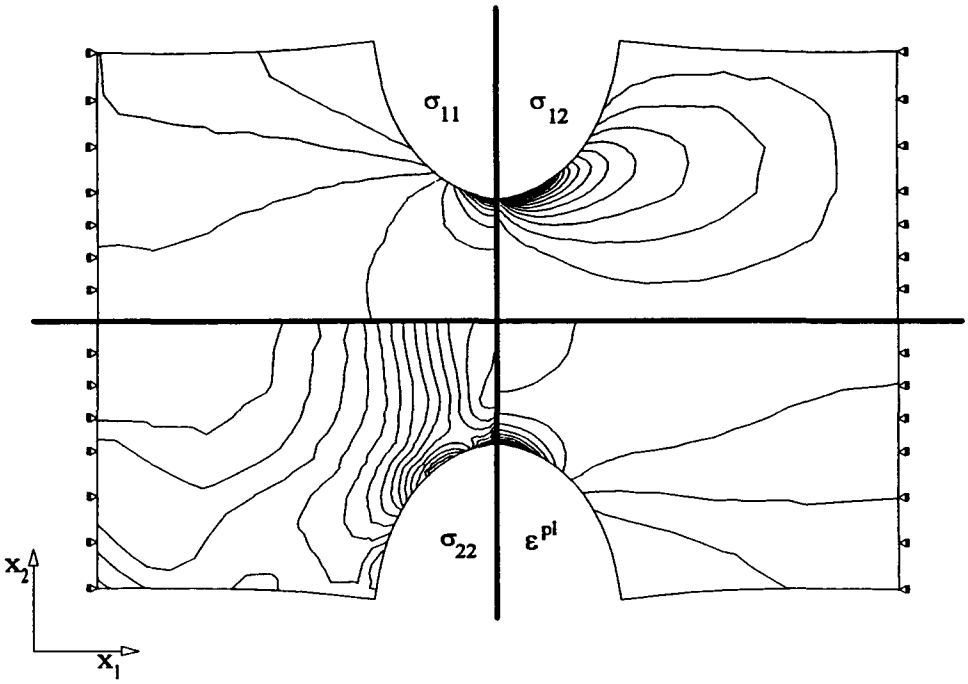

Fig. 7. Plate with elliptical notches (contours of Cauchy stresses and equivalent plastic strain).

REFERENCES

Besdo, D. (1981). Zur Formulierung von Stoffgesetzen der Plastomechanik im Dehnungsraum nach Ilyushin's Postulat. *Ingenieur Archiev* **31,** 1–8.

Bialecki, R., Dallner, R. and Kuhn, G. (1993). New application of hypersingular equations in the boundary element method. *Comp. Meth. Appl. Mech. Engng* **103,** 399–416.

Brebbia, C. A., Telles, J. C. F. and Wrobel, L. C. (1984). *Boundary Element Techniques*. Springer Verlag, Berlin.

Chandra, A. and Mukherjee, S. (1986a). An analysis of large strain viscoplasticity problems including the effects of induced material anisotropy. *J. Appl. Mech.* **53,** 77–78.

Chandra, A. and Mukherjee, S. (1986b). A boundary element formulation for large strain problems of compressible plasticity. *Engng Anal.* **32,** 71–78.

Chen, Z. Q. and Ji, X. (1989). Boundary element analysis of finite deformation problems of elastoplasticity. *Proc. 1st Japan–China Symp. on Boundary Element Methods*, pp. 234–270.

Chen, Z. Q. and Ji, X. (1990). A new approach to finite deformation problems of elastoplasticity boundary element analysis method. *Comp. Meth. Appl. Mech. Engng* **78,** 1–18.

Coleman, B. D. and Gurtin, M. E. (1967). Thermodynamics with internal state variables. *J. Chem. Phys.* **47,** 597–613.

Eterovic, A. L. and Bathe, K. J. (1990). A hyperelastic-based large strain elasto–plastic constitutive formulation with combined isotropic-kinematic hardening using the logarithmic stress and strain measures. *Int. J. Numer. Meth. Engng* **30,** 1099–1115.

Foerster, A. (1993). Eine Boundary Element Formulierung für physikalisch und geometrisch nichtlineare Probleme. Dissertation, Universität Erlangen-Nürnberg.

Foerster, A. and Kuhn, G. (1993). Die Behandlung von großen Deformationen hyperelastischer Materialien mit der Randelementmethode. *Z. Angew. Math. Mech.* **73,** 766–769.

Guiggiani, M., Krishnasamy, G., Rudolphi, T. J. and Rizzo, F. J. (1992). A general algorithm for the numerical solution of hypersingular boundary integral equations. *ASME J. Appl. Mech.* **59,** 604–614.

Haupt, P. (1985). On the concept of an intermediate configuration and its application to a representation of viscoelastic–plastic material behaviour. *Int. J. Plast.* **8,** 303–316.

Hildenbrand, J. and Kuhn, G. (1988). Numerical computation of hypersingular integrals and application to the boundary integral equation for the stress tensor. *Engng Anal. Bound. Elem.* **10,** 209–217.

Jin, H., Mattiasson, K., Runesson, K. and Samuelsson, A. (1988). On the use of the boundary element method for elastoplastic large deformation problems. *Int. J. Numer. Meth. Engng* **25,** 165–176.

Jin, H., Runesson, K. and Mattiasson, K. (1989). Boundary element formulation in finite deformation plasticity using implicit integration. *Comput. Struct.* **31,** 25–34.

Lee, E. H. (1969). Elastic–plastic deformation at finite strains. *J. Appl. Mech.* **36,** 1–6.

Lubliner, J. (1984). A maximum-dissipation principle in generalized plasticity. *Acta Mech.* **52,** 225–237.

Lubliner, J. (1987). Non-isothermal generalized plasticity, *Thermomechanical Couplings in Solids*. (Edited by H. D. Bui and Q. S. Nguyen). Elsevier Science Publishers B.V., IUTAM.

Marsden, J. E. and Hughes, T. J. R. (1983). *Mathematical Foundations of Elasticity*. Prentice-Hall, Englewood Cliffs.

Miehe, C. and Stein, E. (1992). A canonical model of multiplicative elasto-plasticity: formulation and aspects of the numerical implementation. *Eur. J. Mech. A/Solids* **11,** 25–432.

Mukherjee, S. and Chandra, A. (1984). Boundary element formulations for large strain–large deformation problems of plasticity and viscoplasticity. In *Developments in Boundary Element Methods*, Vol. 3, pp. 27–58. Elsevier Applied Science Publications, Amsterdam.

Novati, G. and Brebbia, C. A. (1982). Boundary element formulation for geometrically nonlinear elastostatics. *Appl. Math. Model.* **6,** 136–138.

Okada, H., Rajiyah, H. and Atluri, S. N. (1988). Some recent developments in finite-strain elastoplasticity using the field-boundary element method. *Comput. Struct.* **30,** 275–288.

Okada, H., Rajiyah, H. and Atluri, S. N. (1989). Non-hyper-singular integral-representations for velocity (displacement) gradients in elastic/plastic solids (small or finite deformations). *Comp. Mech.* **4,** 165–175.

Okada, H., Rajiyah, H. and Atluri, S. N. (1990). A full tangent stiffness field-boundary element formulation for geometric and material nonlinear problems of solid mechanics. *Int. J. Numer. Meth. Engng* **29,** 15–35.

Simo, J. C. (1984). Remarks on rate constitutive equations for finite deformation problems: computational implications. *Comp. Meth. Appl. Mech. Engng* **46,** 201–215.

Simo, J. C. (1988a). A framework for finite strain elastoplasticity based on maximum plastic dissipation and the multiplicative decomposition. Part I: continuum formulation, *Comp. Meth. Appl. Mech. Engng* **66,** 199–219.

Simo, J. C. (1988b). A framework for finite strain elastoplasticity based on maximum plastic dissipation and the multiplicative decomposition. Part II: computational aspects. *Comp. Meth. Appl. Mech. Engng* **68,** 1–31.

Simo, J. C. and Miehe, C. (1992). Associative couple thermoplasticity at finite strains: formulation, numerical analysis and implementation. *Comp. Meth. Appl. Mech. Engng* **98,** 41–104.

Stippes, M. and Rizzo, F. J. (1977). A note on the body force integral of classical elastostatics. *Z. Angew. Math. Phys.* **28,** 339–341.

Tran-Cong, T., Zheng, R. and Phan-Thien, N. (1990). Boundary element method for finite elasticity. *Comp. Mech.* **6,** 205–219.

Vogel, S. K. and Rizzo, F. J. (1973). An integral equation formulation of three dimensional anisotropic elastostatic boundary value problems. *J. Elast.* **3,** 203–216.